

Kinetic Model for TiO₂ Polymorphic Transformation from Anatase to Rutile

*Giridhar Madras**

Department of Chemical Engineering, Indian Institute of Science,
Bangalore 560012. India.

Benjamin J. McCoy

Department of Chemical Engineering and Materials Science,
University of California at Davis, Davis, California 95616.

Alexandra Navrotsky

Thermochemistry Facility and NEAT ORU and
Department of Chemical Engineering and Materials Science,
University of California at Davis, Davis, California 95616.

Original ms submitted to *J. Am. Ceram. Soc.* May 9, 2006.

Revised ms submitted Aug. 19, 2006.

* Corresponding author. Phone: 91-80-22932321, Fax: 91-80-23600683.

Email: giridhar@chemeng.iisc.ernet.in

Abstract

We propose a distribution kinetics model for the polymorphic transformation (anatase to rutile) and coarsening of TiO_2 . Based on population balance equations for the size distributions of the dimorphs, the simplified model applies a first-order rate expression for transformation combined with Smoluchowski coalescence for coarsening of anatase and rutile particles. Two moments of the size distributions (number and mass of particles) lead to dynamic expressions for extent of reaction and average particle diameter. The model describes the time-dependent data of Banfield and coworkers [*Am. Mineralogist* **84**, 528-535 (1999); *J. Mater. Res.* **15**, 437-448 (2000)] fairly accurately, and provides activation energies for anatase coalescence and transformation. The equilibrium constant for the microscopically reversible transformation, occurring without coarsening, yields a small endothermic enthalpy change per mole of TiO_2 . This probably reflects contributions of the transformation enthalpy of the anhydrous phases at the given particle size, which is very close to zero, and the enthalpy associated with a small amount of dehydration (endothermic water evaporation) during transformation.

Keywords: solid-solid transformations, polymorph, titania, rutile, anatase

Introduction

Nanocrystalline TiO_2 having the anatase structure is an important material in geology, chemical engineering, and materials science. It undergoes a polymorphic transformation to rutile at high temperatures¹. This transformation has been studied intensively^{2,3,4}, providing a test case for evaluating concepts of polymorphic transformation kinetics and dynamics in metal oxides. Recent experimental and kinetic studies by Banfield and coauthors^{2,3,4} present detailed data for reaction extent and number and size of anatase and rutile particles at different temperatures. [The brookite form of titania also transforms into the rutile phase, sometimes with anatase as an intermediate¹](#). At high temperatures, ultrafine TiO_2 nanoparticles dehydrate and coarsen as they transform from anatase to rutile. The overall process (phase transformation, water loss, and coarsening) is irreversible. This coarsening occurs by coalescence, unlike ripening by recrystallization, which takes place via dissolution of smaller particles and molecular (or ionic) deposition from solution onto larger particles⁵. This latter process can also yield polymorphic transformations, but by a distinctly different mechanism⁶.

Solution calorimetric studies of anatase, brookite (another polymorph) and rutile of different surface areas¹ have shown that the competition of surface energy and transformation energy result in a crossover of thermodynamic stability (in terms of enthalpy and likely also free energy) at the nanoscale, anatase becoming thermodynamically stable at small particle size. Thus the transformation process itself, at a given particle size (without coarsening), may be thermodynamically driven and, conceivably, reversible. It may also be accompanied by a small loss of adsorbed water. The overall irreversibility of the process, however, probably results from continued dehydration and coarsening.

The interplay of kinetics and thermodynamics complicates the dynamics of coalescence-influenced transformation yet makes the analysis particularly interesting. Thermodynamic equilibrium at constant T and P is achieved when the Gibbs free energy is minimized. At the macroscopic level this implies the interfacial energy is minimized by complete coalescence of the particles. For ripening by recrystallization⁶, only when all the particles have recrystallized into a single large particle will true equilibrium be accomplished. When only a few large particles remain, the kinetic driving force may be so small that an essentially infinite time is required before the final equilibrium is attained. Similarly for coarsening by coalescence of TiO₂ in the present work, interfacial energy influences may become negligible after a time when a few large particles remain unagglomerated. In effect, especially if kinetic energy barriers must be overcome, the transition is kinetically arrested and the polymorphic transformation may never occur. As in the glassy state, thermodynamic equilibrium may never be accomplished.

When many small (nano) particles of anatase are present initially, they can transform to rutile only when that reaction lowers the free energy. As argued by several authors^{7,8,9}, the competition among surface energy and the energetics of polymorphism stabilize anatase at smaller particle size, resulting in a crossover in thermodynamic stability at some particle size or surface area. Transformation can occur only at that or larger particle size, with a zero or slightly negative thermodynamic driving force. Thus, when phase transformation occurs faster than coarsening, it takes place under conditions representing a local equilibrium or near equilibrium condition, though this state is metastable and not the global equilibrium state of minimum free energy (coarse or single crystal rutile). Our model addresses this local

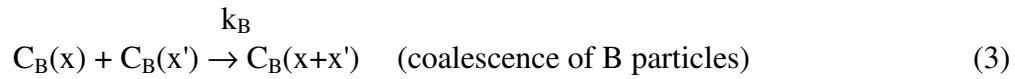
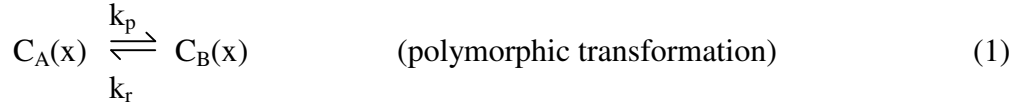
equilibrium between anatase and rutile particles (their adsorbed surface water is an additional complication).

Nanophase particles initially formed from aqueous synthesis are heavily hydrated and not in contact with each other. The types of water form a spectrum ranging from that having the properties of bulk liquid water to a small fraction bound very tightly, probably in the form of hydroxyl groups¹⁰. This tightly bound water is lost at the highest temperature and may take part in the phase transformation. Our physical picture of the transformation is that it occurs independently in each particle, each acting like a large molecule undergoing a chemical reaction. The coalescence/sintering of particles is a separate process, although it determines the number of particles large enough for the transformation to be thermodynamically possible, thus fixing, in a sense, the concentration of reactant. The anatase-rutile transformation is thermodynamically required to be first-order since the two space groups are not related by symmetry¹¹. Furthermore, the structures contain different patterns of octahedral edge sharing, so bonds must be broken during this reconstructive transformation.

Kinetic Model

Separation of the overall process into two steps, reversible polymorphic transformation and irreversible coarsening by coalescence, allows us to model the overall kinetics. We model coalescence by classical Smoluchowski theory and transformation by an overall first-order reaction. The reaction-like transformation approximates the nucleation mechanism, which was previously described in much greater detail by Zhang and Banfield³ as surface, interface, or bulk nucleation. The present model is based on assumptions that the microscopically reversible transformation from A (anatase) to B (rutile) is for ultra-small

particles (and has kinetic parameters independent of size) and that coalescence is the dominating mechanism of coarsening. The reaction-like processes defining the assumed mechanism satisfy TiO_2 mass (x) conservation (apart from water loss),



where k_p and k_r are the first-order rate coefficients for polymorphic transformation from A to B and B to A, respectively. The temperature-dependent parameters, k_A and k_B , are the coalescence rate coefficients for particles A and B. [Equation 1 does not apply to macroscopic thermodynamic equilibrium, but only microscopically under the constraint of initial particle sizes and is effectively a chemical reaction \(with dehydration\) with non-zero heat of transformation.](#)

For continuous distributions the population balance equations^{12,13} are written as time derivatives,

$$\begin{aligned} \partial c_A(x,t)/\partial t = & -2 k_A c_A(x,t) \int_0^\infty c_A(x',t) dx' + k_A \int_0^x c_A(x',t) c_A(x-x',t) dx' \\ & - k_p c_A(x,t) + k_r c_B(x,t) \end{aligned} \quad (4a)$$

and

$$\begin{aligned} \partial c_B(x,t)/\partial t = & -2 k_B c_B(x,t) \int_0^\infty c_B(x',t) dx' + k_B \int_0^x c_B(x',t) c_B(x-x',t) dx' \\ & + k_p c_A(x,t) - k_r c_B(x,t) \end{aligned} \quad (4b)$$

We note that the A particle distribution, $c_A(x,t)$, is mathematically independent of the B particle distribution, $c_B(x,t)$, only if $k_r = 0$. This irreversible case is useful only at high temperatures, where the transformation is nearly complete. The mass moments are defined as

$$c_i^{(n)}(t) = \int_0^\infty c_i(x,t) x^n dx \quad (5)$$

where $n = 0$ and 1 are respectively the number and mass of anatase ($i = A$) and rutile ($i = B$) particles. We define a temperature-dependent equilibrium constant, $K = k_p/k_r$, and apply the integration over x to Eq 4a and 4b to derive the moment equations,

$$dc_A^{(0)}/dt = -k_A c_A^{(0)2} - k_p [c_A^{(0)} - K^{-1} c_B^{(0)}] \quad (6)$$

$$dc_B^{(0)}/dt = -k_B c_B^{(0)2} + k_p [c_A^{(0)} - K^{-1} c_B^{(0)}] \quad (7)$$

$$dc_A^{(1)}/dt = -k_p [c_A^{(1)} - K^{-1} c_B^{(1)}] \quad (8)$$

and

$$dc_B^{(1)}/dt = +k_p [c_A^{(1)} - K^{-1} c_B^{(1)}] \quad (9)$$

It is interesting that Eq 6 with $1/K = 0$, or equivalently $k_r = 0$, is identical to a kinetic rate equation for combined surface and interface nucleation proposed by Zhang and Banfield⁴, who also formulated kinetics in terms of particle numbers³. Assuming coalescence is second-order and transformation first-order in particle numbers immediately gives Eqs 6 and 7 without invoking the population balance equations 4a and 4b. Equations 8 and 9 necessarily follow by mass conservation.

Simultaneous differential Eqs 6 and 7 can be readily solved numerically. For the special case $1/K = 0$ ($k_r = 0$), an analytical solution can be obtained in terms of the initial condition, $c_A^{(0)}(t=0) = c_{A0}^{(0)}$,

$$c_A^{(0)}(t) = c_{A0}^{(0)} \exp(-k_p t) / [1 + (k_A/k_p) c_{A0}^{(0)} (1 - \exp(-k_p t))] \quad (10)$$

Simultaneous Eqs 8 and 9 can be integrated analytically; in terms of the initial conditions,

$c_A^{(1)}(t=0) = c_{A0}^{(1)}$ and $c_B^{(1)}(t=0) = c_{B0}^{(1)}$, the solutions are

$$c_A^{(1)}(t) = c_{A0}^{(1)} (1 + K)^{-1} \{1 + K \exp[-k_p (1 + 1/K) t]\} \quad (11)$$

$$c_B^{(1)}(t) = c_{B0}^{(1)} + c_{A0}^{(1)} - c_A^{(1)}(t) \quad (12)$$

where Eq 12 is a mass balance. The fractional mass conversion is defined³ as

$$\alpha(t) = 1 - c_A^{(1)}(t)/c_{A0}^{(1)} = 1 - (1 + K)^{-1} \{1 + K \exp[-k_p (1 + 1/K) t]\} \quad (13)$$

where Eq 11 has been substituted. The expression for conversion α is thus independent of initial conditions. Rearranging Eq 13 yields

$$-K (1 + K)^{-1} \ln [1 - \alpha (1 + 1/K)] = \chi = k_p t \quad (13a)$$

where χ , defined as the left-hand side of Eq 13a, involves the anatase weight fraction. The average particle mass is the ratio of first to zeroth moments,

$$c_A^{avg}(t) = c_A^{(1)}/c_A^{(0)} \quad (14)$$

and is related to the average diameter D_A^{avg} of the spherical A particles by

$$D_A^{avg}/D_{A0}^{avg} = [c_A^{avg}(t)/c_{A0}^{avg}]^{1/3} \quad (15)$$

in terms of the initial value, $D_A^{avg}(t=0) = D_{A0}^{avg}$. Equation 13 indicates that as $t \rightarrow \infty$, the fractional mass conversion is simply,

$$\alpha(t \rightarrow \infty) = (1 + 1/K)^{-1} \quad (16)$$

The equilibrium constant, K , increases with temperature due to the endothermic dehydration accompanying transformation. Experiments⁴ with anatase diluted with inert alumina powder show how conversion is incomplete when coalescence, and hence coarsening, is inhibited. Particles A (undiluted anatase) are completely converted eventually at higher temperatures so that only coarsened B (rutile) particles remain. Thermodynamic calculations based on calorimetric data predict for coarse material that rutile is the only stable

phase at any temperature below melting while anatase and brookite are metastable. Both thermodynamic¹ and kinetic^{2,3} studies of samples of different particle size suggest, however, for TiO₂ crystals less than a few tens of nanometers in diameter, anatase is more stable than rutile due to surface energy effects. The experimental data^{1,2} and theoretical calculations^{2,3} clearly demonstrate that the stabilities of anatase and rutile reverse when surface energy contributions to total free energy are significant and this makes anatase the stable phase at very small crystallite sizes.

Results and Discussion

The data published by Banfield and coworkers^{2,3,4} show distinctive features that must be predicted by a valid model. For the transformation of nanocrystalline anatase to rutile, several kinetic models have been shown^{2,3} unable to interpret experimental data, including models for the standard first-order reaction^{14,15}, standard second-order reaction¹⁶, contracting spherical interface¹⁷, nucleation and growth of overlapping nuclei^{1414149,17171712}, one-dimensional linear and branching nuclei and constant growth¹⁴¹⁴¹⁴⁹, random nucleation and rapid growth,^{1414149,17171712} and the universal Johnson-Mehl-Avrami-Kolmogorov (JMAK) approach.^{17171712,18} A proposed interface nucleation model² satisfactorily described the transformation kinetics of nano-crystalline anatase samples in the temperature range 738 – 798 K, and in order to interpret data at higher temperatures, 893 – 963 K, the model was revised³ to incorporate surface nucleation. In the current work, we show that the single model based on distribution kinetics reasonably represents the experimental data over the entire temperature range from 738 to 963 K. [The proposed model thus has the advantage of reducing the number of parameters needed to describe quantitatively the observed behavior.](#)

The equilibrium constant K is estimated for extrapolated data of the final fractional mass conversion (Table 1), as indicated by Equation 16. Even though the limiting final conversion can be obtained only in the idealized absence of coarsening, the data of Fig. 1 in Ref. 3 for 738 K show that after 800 h the transformation reaches 50 percent. With values of K , Eq 13a indicates a linear plot of χ versus t can be obtained with a slope of k_p . The experimental data^{3,4} (Fig 2 of Ref. 3 and Fig. 1a of Ref. 4) of the fraction mass conversion, and the linear regression are shown in Figures 1a and 2a. Including the reversible reaction (1) is consistent with the experimental evidence and is necessary, because for an irreversible reaction, $1/K = 0$ and a plot of $\ln(1 - \alpha)$ versus t would be linear, which is known² not to be valid except for very high temperature data.

The time variation of the average particle size of anatase is obtained by solving Eqs 6 and 7 numerically for the zeroth moment. Then, using the expression for the first moment (Eq 11), one substitutes into Eq 14. The numerical solution obtained by Mathematica® was verified with the analytical solution for the special case of $1/K = 0$. With the value of K determined from Eq 16 and the regressed k_p (obtained from Figures 1a and 2a) the value of k_A is obtained by nonlinearly regressing the experimental data^{3,4} (Fig. 7 of Ref. 3 and Fig. 1b of Ref. 4) for the variation with time of the average particle size of anatase at various temperatures (Fig. 1b and 2b). Solving Eqs 6 and 7 simultaneously for $c_A^{(0)}$ and $c_B^{(0)}$ requires values of both k_A and k_B , which were assumed related by $k_B = 0.10 k_A$. The inflection observed in Fig 2b is due to the variation of the zeroth moment, which rapidly approaches zero. To verify this, we simulated the experimental data³ (Fig. 3 of Ref. 3) of the variation of the zeroth moment (corresponding to the number of particles of anatase) at various temperatures T (Figure 1c) using the same parameter values. The satisfactory fit of the model

to a wide variety of experimental data supports the validity of the model. The number of anatase particles initially decreases sharply and vanishes at longer times. The fractional transformation to rutile, α , increases to equilibrium conversion, which is unity at very high temperature. Rates obeying Arrhenius temperature dependence are enhanced at higher temperatures. The simple model presented here is able to capture all the above characteristics of solid-solid transformations and is applicable at all temperatures.

Only one major adjustable parameter, k_A , appears in the analysis. The value of K is determined from the long-time asymptote observed in experimental data and k_p is obtained from the linear regression of the straight lines in Figures 1a and 2a. The value of k_A is obtained by nonlinearly regressing the experimental data values. The value of k_B is assumed to be related by $k_B = 0.10 k_A$. A sensitivity analysis for the data at 798 K justifies the assumption and the regression procedure to determine k_A . Changing the value of k_A has a significant effect on the time evolution of the average sizes; increasing or decreasing k_A by a factor of two causes up to 35 percent change in the particle size ratio. The effect of the assumption $k_B = 0.10 k_A$ proves to have essentially a negligible effect on the particle size ratio.

Equation (1) is written as an equilibrium or chemical reaction, with forward and reverse rate constants whose ratio defines an equilibrium constant. One might question whether such a formalism is appropriate for a solid-solid phase transformation. We believe it is because each TiO_2 particle (and its associated water) is in fact behaving like a large molecule or cluster during the transformation. Because transformation is faster than agglomeration, coarsening, or sintering, the former and not the latter determines the local equilibrium. A given particle (molecule) transforms very quickly; there is no evidence of a

particle remaining partially transformed, and indeed it is likely that the transformation, once it starts, sweeps rapidly through the particle, which is too small to harbor planar defects like grain boundaries or dislocations, which would sweep out to the surface. The rates of transformation reflect the number of particles transforming in unit time. Indeed the model is formulated in terms of numbers (or moles) of particles, not moles of TiO₂. Thus in a sense the model treats the particles as each representing a large molecule. Nevertheless, the overall transformation is first-order and has a latent heat (see below).

We next show that our model yields the correct trends when the initial particles are either diluted (as by alumina) or compacted (Figure 3a). One decreases or increases, respectively, the initial number concentration (zeroth moment) and mass concentration (first moment) such that the initial diameter (size) is the same. The number concentration and average diameter change in the expected way: dilution decreases all the rates and compaction increases the rates. The results show that the evolution of particle size depends on whether anatase particles are aggregated or separated. The assumed first-order transformation is consistent with the conclusion of previous work¹⁹, which suggested that the rutile phase starts to form at the interfaces between the anatase particles in the agglomerated TiO₂ particles. This suggests that the nucleation occurs within a single particle already coalesced, hence, first-order transformation is realistic. It is likely that coalescence (agglomeration) is not an instantaneous event, and consolidation of the aggregated particles proceeds with time after the particles initially contact via aggregation. This would allow nucleation at the interfaces between regions in the already aggregated particles, consistent with structural analysis and TEM observations¹⁹⁺¹⁹¹⁴.

We also show that the model fits the experimental data of the time evolution for number concentration and average diameter in the presence of alumina. Experimental data⁴ indicate that the transformation and coarsening of anatase particles are retarded when the sample is intimately mixed with alumina. The influence of alumina on the final particle size obtained is larger than the effect of temperature, indicating that the number of contacting anatase particles is reduced by the added alumina, thus reducing interface nucleation. Because alumina influences the kinetic parameters of coalescence and the reaction, the values of k_p and K are different from those in Table 1. Thus with $k_p = 0.0195 \text{ min}^{-1}$ and $K = 6.71$, the model provides a satisfactory fit to the experimental data for the fractional transformation of anatase to rutile and for the time evolution of the average size of anatase particles in presence of alumina (Fig. 3b and 3c) at 913 K. Only one temperature is included here because the data at the other temperature are quite scattered and show anomalous behavior.

Figure 4, based on Table 1, shows temperature effects as Arrhenius plots for the rate coefficients, k_A and k_p , and the equilibrium constant, K . The rate coefficient expressions, determined from the slopes of the linearly regressed Arrhenius plots, are $\ln k_A = 39.8 - 32870/T$ and $\ln k_p = 31.8 - 31330/T$. Activation energies for k_A and k_p are thus $E_A = 273$ and $E_p = 260$ kJ per mole of particles, respectively, smaller than the exceptionally large values reported in other studies³. The equilibrium constant determined from the slope in Fig. 3 is $\ln K = 23.6 - 17700/T$, thus $\Delta\Delta H = +147$ kJ per mole of particles.

This large positive enthalpy of transformation per mole of particles seems surprising at first glance, in both sign and magnitude. The enthalpy of the anatase to rutile transformation is small and exothermic (-2.6 ± 0.4 kJ/mol) for bulk samples¹. However, the ΔH of transformation calculated here refers to the near-equilibrium transformation at a particle size

near the energetic crossover inferred from calorimetric data¹. Assuming reversibility (ΔG of transformation is zero or, since this assumption of reversibility is an approximation, ΔG is near zero), one can say that a small value of ΔH , either positive or negative, is possible as the particles are transforming, especially since one expects ΔS of transformation, both for bulk material and for nanoparticles, to be small in magnitude, but does not know its sign. Thermodynamically, if the reaction is reversible at the nanoscale and rutile is indeed the high temperature phase, then ΔH and ΔS of the overall reaction must be positive. The samples contain adsorbed water, a small amount of which is probably released during the transformation. This enthalpy is on the order of 45-60 kJ per mole of H_2O at room temperature, depending on whether the water is bound more strongly than physisorbed liquid water. Thus an overall endothermic enthalpy associated with the transition is plausible.

Is the magnitude reasonable? Since we have ignored the effect of particle size on the thermodynamic and kinetic parameters, we can only present a very approximate calculation. For particles with a diameter of d , the number of particles per mole of substance is $N_A d^3 \rho / 6M$, where N_A is Avogadro's number, ρ is the density, and M the molecular weight. For 10 nm particles, a molecular weight of 80 and a density of 3.84 g/cm^3 for anatase, this gives 15,000 particles per mole of TiO_2 . The enthalpy of transformation per mole of TiO_2 is then $147/15000 = 0.01 \text{ kJ/mol}$, a small value indeed. As long as the $T\Delta S$ term is small, this confirms that the transformation is occurring at or near equilibrium. If the particle size is 100 nm, ΔH is 10 kJ per mol of TiO_2 . Since at the point of transformation in the experimental system, most particles are well under 100 nm in diameter, the argument presented here is applicable to the real experimental system.

The equilibrium constant K , linking kinetics to energetics, determines the direction (forward or reverse) and extent of the reaction (1). Ranade et al.¹ summarized the energetics of nanocrystalline TiO_2 , in particular, the influence of particle size. The present model, by assuming K is independent of particle size, suggests that the transformation kinetics would be complicated by the size dependence of energetics. Slight deviations from linearity in Figs. 1a and 2a may be attributed to this approximation. When enthalpy, and hence free energy, depends on particle size, a mechanism-based, distribution-kinetics model formulated as differential equations does not seem feasible. Numerical solutions for population balance equations for the size distributions, however, may be possible, even when all the relevant phenomena are incorporated.

Along an equilibrium phase boundary, two or more phases may be in equilibrium, for example, two polymorphs in a single component system, three phases at a triple point in a single component system, and two phases of different compositions in a binary solid solution loop. Once interfaces and very small particles are brought into play, the situation becomes even more complex, and the system can be in a series of constrained equilibrium states, for instance, at constant number of atoms per particle. The process is intermediate between that of large molecular clusters in solution (to which Eq. 1 clearly applies) and bulk crystalline solids in which surface effects can be neglected and the Gibbs phase rule can be applied in a classical sense. Once hydration is considered, the two types of particles, A and B, are no longer even of the same composition. In our interpretation the reversible transformation from A to B is effectively a chemical reaction with nonzero heat of transformation. The release of H_2O (dehydration) during the transformation further supports this view. The ratio $K = k_p/k_r$ is a local, microscopic equilibrium constant that refers to the transformation as it is occurring,

not to the final state of lowest free energy, namely coarse rutile. Equation 1 thus applies, not for macroscopic thermodynamic equilibrium, but only microscopically under the constraint of the initial particle sizes. The proposed model differs from other approaches by combining microscopic Eq 1 with the observed macroscopic coalescence processes of Eqs 2 and 3.

More data on time evolution of particle diameters and concentration for different systems of polymorphic transformation would help in testing this and other models. Experimental data on the effect of hydration, particle sizes, and dilution on the kinetics of the system would provide insights into the mechanisms involved in the polymorphic transformations.

Conclusion

In this work, we have distinguished coarsening by coalescence from ripening by recrystallization. Coalescence is modeled by classical Smoluchowski theory and transformation is assumed an overall first-order reaction. This assumption approximates the nucleation process, which was previously described by detailed mechanisms³. The new model is based on population balance equations for the time-dependent mass distributions of anatase and rutile. The lowest mass moments of the distributions, the numbers and masses of the dimorphs, satisfy differential equations for the time evolution of the coalescence and transformation (anatase to rutile). Arrhenius temperature plots for the coalescence and transformation rate coefficients yield reasonable activation energies for metal oxides. Our model quantitatively explains published experimental data for transformation between the dimorphs anatase and rutile, and can be readily generalized to transformations among three or more polymorphs.

Acknowledgments

This work was supported by the U.S. Department of Energy (Grant DE-FG02-05ER15667). We thank Dr. H. Zhang for valuable discussions.

References

- ¹ M.R. Ranade, A. Navrotsky, H. Z. Zhang, J. F. Banfield, S. H. Elder, A. Zaban, P. H. Borse, S. K. Kulkarni, G. S. Doran and H. J. Whitfield, "Energetics of nanocrystalline TiO₂", *PNAS* 99, Suppl. 2, 6476-6481 (2003).
- ² A.A. Gribb, J.F. Banfield, "Particle size effects on transformation kinetics and phase stability in nanocrystalline TiO₂," *Am. Mineralogist*, **82**, 717-728 (1997).
- ³ H. Zhang, J.F. Banfield, "New kinetic model for the nanocrystalline anatase-to-rutile transformation revealing rate dependence on number of particles," *Am. Mineralogist*, **84**, 528-535 (1999).
- ⁴ H. Zhang, J.F. Banfield, "Phase transformation of nanocrystalline anatase-to-rutile via combined interface and surface nucleation," *J. Mater. Res.*, **15**, 437-448 (2000).
- ⁵ B. Gilbert, H. Zhang, F. Huang, M.P. Finnegan, G.A. Waychunas, J.F. Banfield, "Special phase transformation and crystal growth pathways observed in nanoparticles," *Geochem. Trans.*, **4**, 20 (2003).
- ⁶ G. Madras, B.J. McCoy, "Growth and ripening kinetics of crystalline polymorphs," *Crystal Growth & Design*, **3**, 981-990 (2003).
- ⁷ [R. C. Garvie. "The occurrence of metastable tetragonal zirconia as a crystallite size effect," *J. Phys. Chem.* **69**, 1238-1243 \(1965\).](#)
- ⁸ [H. Zhang and J. F. Banfield, "Understanding polymorphic phase transformation behavior during growth of nanocrystalline aggregates: insights from TiO₂," *J. Phys. Chem. B*, **104**, 3481-3487 \(2003\).](#)

⁹ [A. Navrotsky, "Energetics of nanoparticle oxides: interplay between surface energy and polymorphism," *Geochemical Transactions* **4**, 34-37 \(2003\).](#)

¹⁰ [A. A. Levchenko, G. Li, J. Boerio-Goates, B. F. Woodfield, A. Navrotsky, "TiO₂ energy landscape: polymorphism, surface energy, and bound water energetics," *Chem. Mater.* \(submitted\).](#)

¹¹ [L.D. Landau, E.M. Lifshitz, *Statistical Physics, 2nd Ed.*, Addison-Wesley, Reading, \(1969\); Chaps. 13, 14.](#)

¹² G. Madras, B.J. McCoy, "Distribution kinetics of Ostwald ripening at large volume fraction and with coalescence," *J. Colloid Interface Sci.* **261**, 423-433 (2003).

¹³ G. Madras, B.J. McCoy, "Reversible crystal growth-dissolution and aggregation-breakage: numerical and moment solutions for population balance equations," *J. Powder Technology.* **143**, 297-307 (2004).

¹⁴ F.C. Gennari and D.M. Pasquevich, "Kinetics of the anatase rutile transformation in TiO₂ in the presence of Fe₂O₃," *J. Mater. Sci.*, **33**, 1571 (1998).

¹⁵ C.N.R. Rao, "Kinetics and thermodynamics of the crystal structure transformation of spectroscopically pure anatase to rutile," *Can. J. Chem.*, **39**, 498 (1961).

¹⁶ A.W. Czanderna, C.N.R. Rao, and J.M. Honig, "The Anatase-Rutile Transition .1. Kinetics Of The Transformation Of Pure Anatase." *Trans. Faraday Soc.*, **54**, 1069 (1958).

¹⁷ R.D. Shannon and J.A. Pask, "Kinetics of the Anatase-Rutile Transformation", *J. Am. Ceram. Soc.*, **48**, 391 (1965).

-
- ¹⁸ K.N.P. Kumar, K. Keizer, and A.J. Burggraaf, "Textural Evolution and Phase Transformation in Titania Membranes: Part 1. Unsupported Membranes," *J. Mater. Chem.*, **3**, 1141 (1993).
- ¹⁹ J. Zhang, M. Li, Z. Feng, J. Chen, and C. Li, "UV Raman spectroscopic study on TiO₂. I. Phase transformation at the surface and in the bulk," *J. Phys. Chem. B*, **110**, 927 (2006).

Table 1. Regressed rate coefficients k_p and k_A at different temperatures T . The equilibrium coefficient K was obtained by fitting final fractional mass conversion (Eq 16) from the indicated data^{3,4}.

| T/K | k_p/min^{-1} | $k_A/\text{vol.}\cdot\text{mol}^{-1}\text{min}^{-1}$ | K | K was obtained by fitting long-time data of |
|-----|-----------------------|--|------|---|
| 738 | 3.33×10^{-5} | 1.33×10^{-2} | 1.19 | Fig 2 of Ref. 3 |
| 753 | 7.00×10^{-5} | 2.80×10^{-2} | 1.39 | Fig 2 of Ref. 3 |
| 773 | 1.32×10^{-4} | 5.27×10^{-2} | 1.60 | Fig 2 of Ref. 3 |
| 798 | 3.25×10^{-4} | 0.13 | 2.0 | Fig 2 of Ref. 3 |
| 893 | 2.29×10^{-2} | 22.9 | 30.5 | Fig. 1a of Ref. 4 |
| 913 | 6.05×10^{-2} | 48.4 | 41.5 | Fig. 1a of Ref. 4 |
| 933 | 2.78×10^{-1} | 111. | 170. | Fig. 1a of Ref. 4 |
| 963 | 6.10×10^{-1} | 305. | 289. | Fig. 1a of Ref. 4 |

Figure Captions

Figure 1. Time dependence of (a) variable for anatase weight fraction, (b) average particle size, and (c) number of anatase particles at temperatures 738 – 798 K. The points represent experimental data³ and the lines are based on the current model (Eqs 13a and 15).

Figure 2. Time dependence of (a) variable for anatase weight fraction and (b) average particle size at temperatures 893 – 963 K. The points represent experimental data⁴ and the lines are based on the current model (Eqs 13a and 15).

Figure 3. Time dependence of the average particle size at temperature 913 K with (a) dilution and compaction and (b) in presence of alumina. Figure 3c shows the time dependence of the variable χ for anatase weight fraction in presence of alumina. The points represent experimental data⁴ and the lines are based on the current model (Eqs 13a and 15).

Figure 4. Arrhenius plots of the equilibrium constant (K) and rate coefficients for coalescence (k_A) and transformation (k_p) over the temperature range, 738 – 963 K.

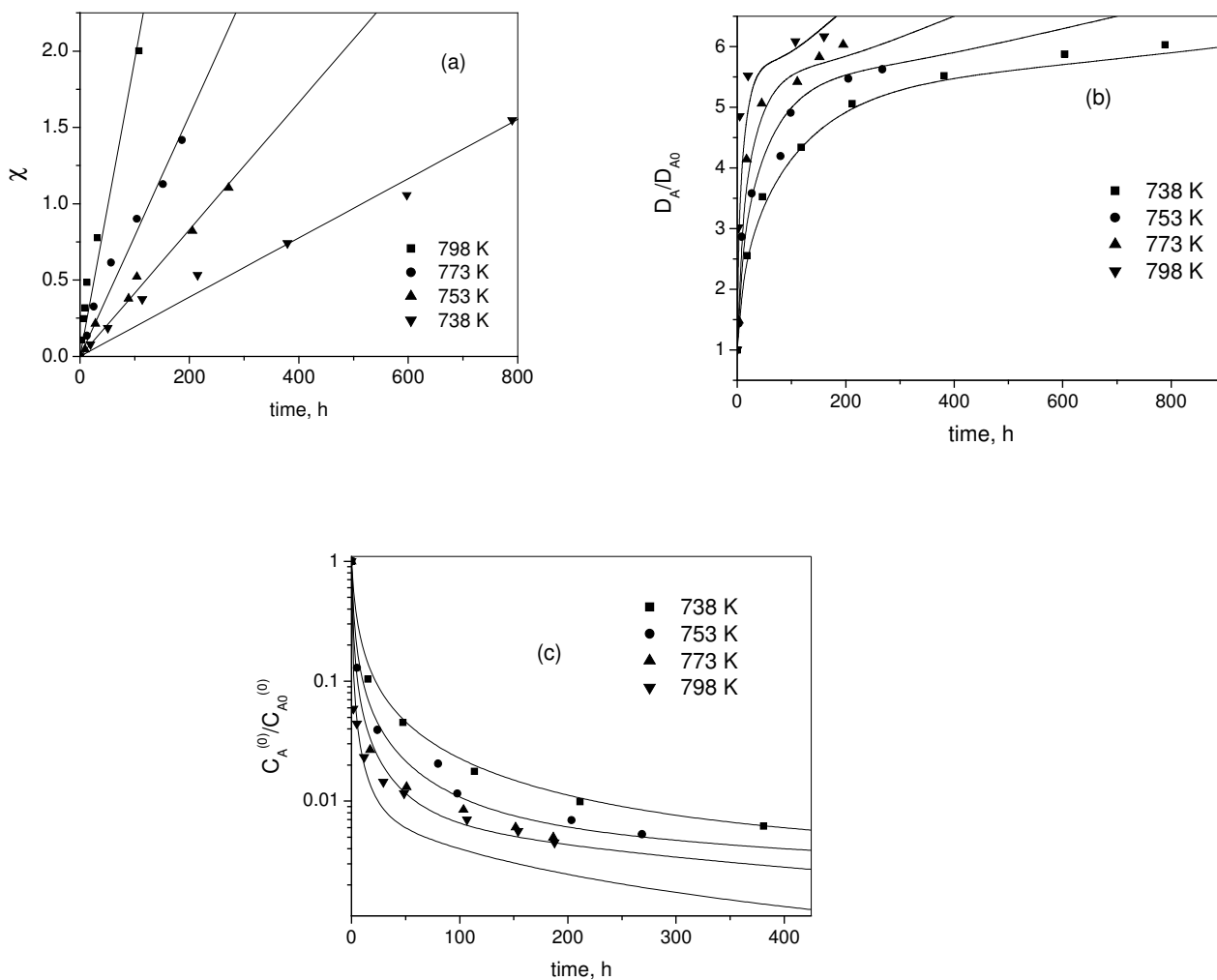


Figure 1. Time dependence of (a) variable for anatase weight fraction, (b) average particle size, and (c) number of anatase particles at temperatures 738 – 798 K. The points represent experimental data³ and the lines are based on the current model (Eqs 13a and 15).

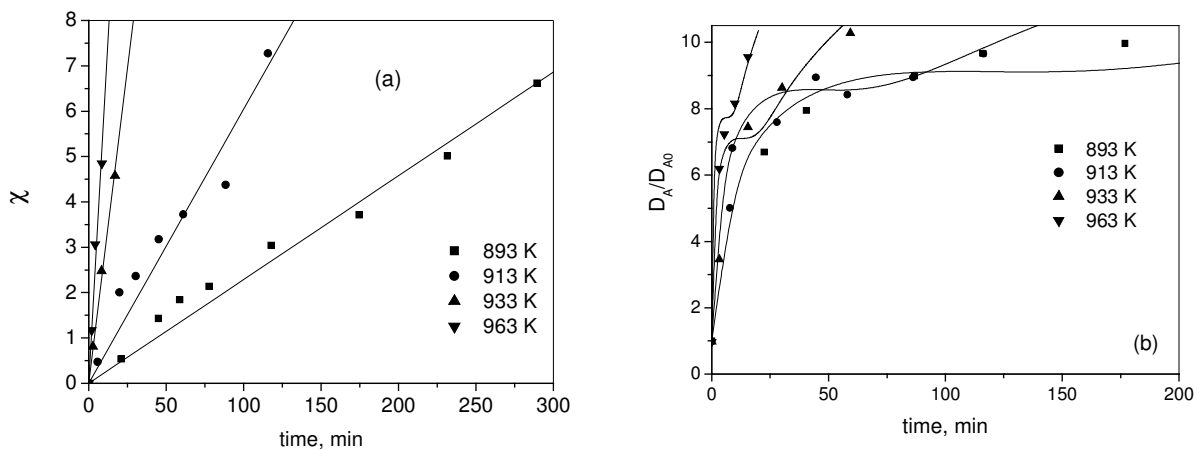


Figure 2. Time dependence of **(a)** variable for anatase weight fraction and **(b)** average particle size at temperatures 893 – 963 K. The points represent experimental data⁴ and the lines are based on the current model (Eqs 13a and 15).

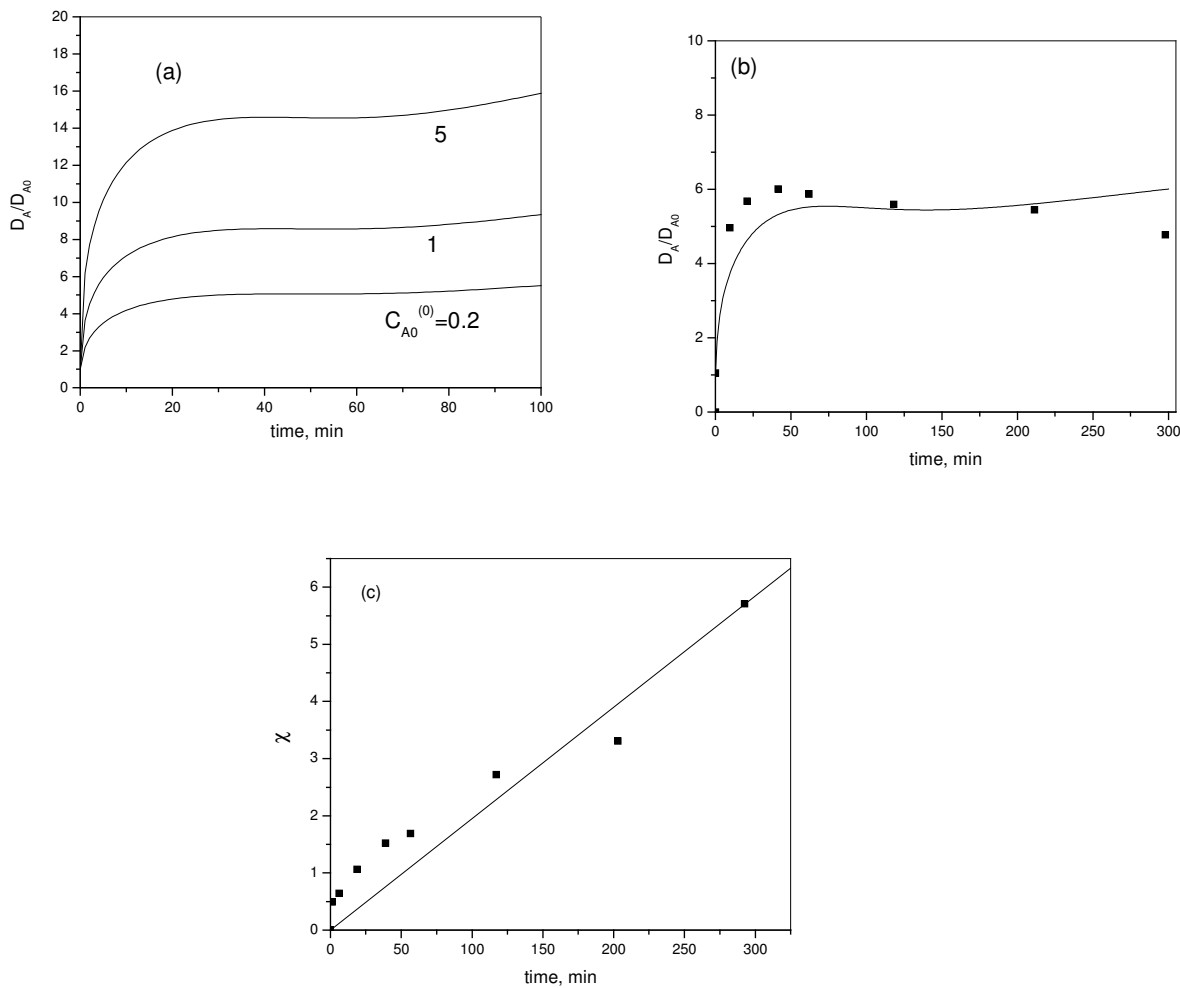


Figure 3. Time dependence of the average particle size at temperature 913 K with (a) dilution and compaction and (b) in presence of alumina. Figure 3c shows the time dependence of the variable χ for anatase weight fraction in presence of alumina. The points represent experimental data⁴ and the lines are based on the current model (Eqs 13a and 15).

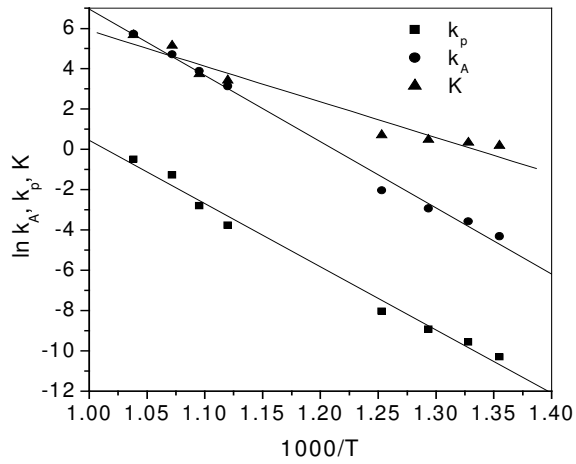


Figure 4. Arrhenius plots of the equilibrium constant (K) and rate coefficients for coalescence (k_A) and transformation (k_p) over the temperature range, 738 – 963 K.